

Direct Observation of Longitudinally Polarised W^\pm Bosons

The L3 Collaboration

Abstract

The three different helicity states of W^\pm bosons, produced in the reaction $e^+e^- \rightarrow W^+W^- \rightarrow \ell\nu q\bar{q}$ are studied using leptonic and hadronic W decays at $\sqrt{s}=183$ GeV and 189 GeV. The W polarisation is also measured as a function of the scattering angle between the W^- and the direction of the e^- beam. The analysis demonstrates that W bosons are produced with all three helicities, the longitudinal and the two transverse states. Combining the results from the two center-of-mass energies and with leptonic and hadronic W decays, the fraction of longitudinally polarised W^\pm bosons is measured to be $0.261 \pm 0.051(\text{stat.}) \pm 0.016(\text{syst.})$ in agreement with the expectation from the Standard Model.

Submitted to *Phys. Lett. B*

Introduction

Previous measurements of W^+W^- production at LEP have concentrated on measurements of the W mass, the W branching ratios, the differential and total cross sections and the anomalous couplings [1–3]. These measurements show, using the differential cross sections with respect to the W production and decay angles, good agreement with theoretical calculations within the Standard Model [4,5]. This good agreement with the Standard Model indicates indirectly that W bosons with all three helicities are produced in the reaction $e^+e^- \rightarrow W^+W^-$.

The primary goal of the measurement described in this paper is a quantitative and model independent analysis of all three W helicity states and in particular, the direct observation of longitudinally polarised W bosons. Measurements of longitudinally polarised W bosons have previously been reported in the reaction $e^+e^- \rightarrow W^+W^-$ [3] and in top decays [6].

At center-of-mass energies close to 190 GeV and within the Standard Model, one expects that about one quarter of all W bosons should be longitudinally polarised [7]. Furthermore, the production of W bosons with different helicities depends strongly on the W^- scattering angle θ_{W^-} with respect to the e^- beam direction. For example one expects for θ_{W^-} larger than 90 degrees that almost 40% of the events contain at least one longitudinally polarised W boson. In contrast, for θ_{W^-} between 20 and 70 degrees, the cross section is dominated by the neutrino-exchange diagram and the W^+W^- should be produced dominantly with transverse polarisation. The fractions of the W^\pm helicity states should thus also be measured as a function of θ_{W^-} .

The measurement is performed with the L3 detector at LEP, using data samples of 55.5 pb^{-1} and 176.4 pb^{-1} collected at average center-of-mass energies of 183 GeV and 189 GeV, respectively. A detailed description of the L3 detector and its performance is given in reference [8]. The L3 detector response for W^+W^- events from the KORALW [9] and the EEWW [10] Monte Carlo programs is simulated with the GEANT-based L3 detector simulation program [11].

Analysis strategy

The different W helicity states result in different angular distributions of the W decay products. The decay angle θ^* in the W rest frame between the left-handed negatively charged lepton and the W^- has a $(1 \pm \cos \theta^*)^2$ distribution for a W^- with helicity ∓ 1 . The right-handed positively charged lepton has a $(1 \pm \cos \theta^*)^2$ distribution for a W^+ with helicity ± 1 . Longitudinally polarised W bosons (helicity 0) result in a symmetric distribution of the decay products, proportional to $\sin^2 \theta^*$. To simplify the description of the helicity fractions, we refer in the following text only to the fractions f_- , f_0 and f_+ of the W^- helicities, which includes the corresponding W^+ states with f_+ , f_0 and f_- , respectively.

In order to study the W polarisation, we use events of the type $e^+e^- \rightarrow W^+W^- \rightarrow \ell^\pm \nu q \bar{q}$ with ℓ^\pm being either e^\pm or μ^\pm . The neutrino four-momentum vector is reconstructed from the total missing momentum vector of the event. These event samples are essentially background free and allow a measurement with good accuracy of the W^\pm momentum vector, the W charge and the decay angle θ^* in the W rest frame.

In contrast to leptonic W decays, where the decay angle θ_ℓ^* of the ℓ^\pm is well defined, the corresponding θ_q^* for quarks in W decays has to be calculated from the hadronic decay products. To approximate the quark decay angle in the W rest frame, we proceed in the following way. First, all particles besides the charged lepton and the missing neutrino in the event are associated with the hadronic decay of the W. We then calculate their associated four-vectors

in the rest frame of the W and determine the corresponding thrust axis in this rest frame. The angle θ_{Thrust}^* of this thrust axis with respect to the W momentum vector in the laboratory frame is used to describe the quark decay angle θ_q^* in the W rest frame.

After correcting for efficiencies, the contributions from different W polarisation states are obtained from a fit to the $\cos \theta^*$ distributions. For the leptonic W decays the fractions f_- , f_+ and f_0 of the three W helicity states are obtained from:

$$\frac{1}{N} \frac{dN}{d \cos \theta^*} = f_- \frac{3}{8} (1 + \cos \theta^*)^2 + f_+ \frac{3}{8} (1 - \cos \theta^*)^2 + f_0 \frac{3}{4} \sin^2 \theta^*. \quad (1)$$

For hadronic W decays, without quark charge identification, one measures only the absolute value of the W hadronic decay angle $|\cos \theta^*|$. However, this distribution can still be used to measure the fractions for the sum of the two transverse helicity states $f_{\pm} = f_- + f_+$ and f_0 using:

$$\frac{1}{N} \frac{dN}{d |\cos \theta^*|} = f_{\pm} \frac{3}{4} (1 + \cos^2 \theta^*) + f_0 \frac{3}{2} \sin^2 \theta^*. \quad (2)$$

The predictions for the compositions of W helicity states as a function of the W^- scattering angle θ_{W^-} , following the formalism of Hagiwara *et al.* [7] and its implementation in the KORALW Monte Carlo program [9], are used as the Standard Model prediction for our analysis. The helicity composition of the total W sample is extracted from a fit to the distribution of the simulated decay angles. From a fit to a KORALW Monte Carlo event sample at $\sqrt{s}=189$ GeV, with a size 100 times larger than the data sample, the Standard Model predictions for inclusive W helicity fractions f_- , f_+ and f_0 are obtained to be 56.3%, 18.0% and 25.7%, respectively. The statistical errors are smaller than 0.5%.

Within the statistical errors, the same fractions are found from a WW event sample generated with the EEWW Monte Carlo program [10] which uses the zero total W width approximation and assigns the W helicities on an event by event basis. The W helicity fractions obtained from the fit to the decay angle distributions agree, within statistical errors smaller than 0.9%, with the generated W helicity fractions. This shows that the Born level formulæ (1) and (2) are applicable after radiative corrections.

Selection of $W^+W^- \rightarrow e(\mu)\nu q\bar{q}$ events

The selection of $W^+W^- \rightarrow e(\mu)\nu q\bar{q}$ events is similar to the selections described in our previous publications on WW final states [1]. However, in order to assure well measured W production and decay angles, more restrictive criteria are used. Charged leptons are identified using their characteristic signatures. Electrons are identified as isolated energy depositions in the electromagnetic calorimeter with electromagnetic shower shape which are matched in azimuth to a track reconstructed in the central tracking chamber. The energy and direction of electrons are measured using the electromagnetic calorimeter, while the charge is obtained from the associated track. Muons are identified and measured with tracks reconstructed in the muon chambers which point back to the interaction vertex. All other energy depositions in the calorimeters are assumed to originate from the hadronic W decay. The neutrino momentum vector is set equal to the total missing momentum vector of the event. In addition the following criteria are used for the selection of $W^+W^- \rightarrow e(\mu)\nu q\bar{q}$ events:

- The reconstructed momentum should be greater than 20 GeV for electrons and 15 GeV for muons.
- The momentum of the neutrino should be greater than 10 GeV and its polar angle, θ_ν , has to satisfy $|\cos \theta_\nu| < 0.95$.
- The invariant mass of the $\ell\nu$ system should be greater than 60 GeV.
- The invariant mass of the hadronic system should be between 50 and 110 GeV.

Using these criteria, 81 and 288 events of the type $W^+W^- \rightarrow e\nu q\bar{q}$ are selected at center-of-mass energies of 183 GeV and 189 GeV, respectively. The corresponding event numbers for $\mu\nu q\bar{q}$ are 67 and 262 events. Adding the electron and muon event samples together, we find 68 and 280 ℓ^- events and 80 and 270 ℓ^+ events, respectively, in the 183 GeV and 189 GeV data samples. These samples have a purity of 96%, where the background from $W^+W^- \rightarrow \tau\nu q\bar{q}$ with leptonic τ decays and the background from $e^+e^- \rightarrow \text{hadrons}$ contribute each about 2%.

The measured $\cos \theta_{W^-}$ distribution is found to be in good agreement with the MC expectations, as shown in Figure 1 for events with electrons and with muons for the 189 GeV data sample. About 5% of the accepted events with electron candidates have a wrongly assigned charge. Charge confusion is insignificant for events with muons. The charge confusion depends on the reconstructed W^- scattering angle and is largest for W bosons with small scattering angle with respect to the beam direction. This results in a small misassignment between W bosons with helicity +1 and -1 but has negligible effects for the fraction of longitudinally polarised W bosons, which is essentially independent of the charge assignment.

Analysis of the W helicity states

After subtracting the backgrounds from the data, the fractions of the W helicity states are measured from the distributions $dN/d \cos \theta_{\ell^\pm}^*$ and $dN/d |\cos \theta_{\text{Thrust}}^*|$ for the leptonic and hadronic W decay angle and as a function of the scattering angle θ_{W^-} .

To extract the W helicity fractions, the observed distributions are corrected for the selection efficiencies which are obtained as a function of $\cos \theta^*$. To take into account possible deviations between the helicity fractions in the data and Monte Carlo as a function of $\cos \theta_{W^-}$, the data are corrected differentially using 9 bins of the $\cos \theta_{W^-}$ scattering angle. For each $\cos \theta_{W^-}$ bin, the efficiency is obtained as a function of $\cos \theta^*$ using the ratio of the reconstructed and the generated $\cos \theta^*$ distributions for the leptonic and hadronic W decays. The measured $\cos \theta^*$ distributions for the corresponding $\cos \theta_{W^-}$ bins in the data are corrected and combined.

The efficiency corrections are obtained from large samples of fully simulated KORALW Monte Carlo events. Using these Monte Carlo events we have studied the accuracy with which we reconstruct the θ^* decay angles. The study shows that θ^* is reconstructed with a standard deviation of 9.2 degrees and a small shift of -3.2 degrees for the leptonic W decays. For hadronic W decays one finds that θ^* is reconstructed with a standard deviation of 12.0 degrees and a shift of +3.3 degrees.

The bias and sensitivity loss due to the efficiency corrections and the θ^* resolution has been determined with fully simulated and reconstructed Monte Carlo events where the generated W helicity fractions have been varied over a large range. This was done both with the EEWW Monte Carlo program, where the generated W helicities are known on an event by event basis

and with the KORALW Monte Carlo using a weighting method to assign the W helicities on a statistical basis, ignoring W spin correlations.

Averaging both Monte Carlo estimates one finds that leptonic W decays with 100% helicity -1 states would be measured to consist of 94% of helicity -1 and 6% helicity 0 states while a W sample with 100% helicity $+1$ would be reconstructed to consist of more than 99% of helicity $+1$ states. Similar numbers are found if one starts with 100% helicity 0, which would be measured with 92% helicity 0, 3% helicity -1 and 5% helicity $+1$. The corresponding numbers for hadronic W decays are that 94% of W bosons with helicity ± 1 and 85% of W bosons with helicity 0 are correctly reconstructed. The study has been repeated as a function of $\cos \theta_{W^-}$ and within the statistical errors the results are the same as the ones from the total W sample. To obtain a correction function for the bias and the efficiency loss, the fraction f_0 has been varied between 0 and 100%. A linear relation between the generated and the fitted W helicity fractions is found.

Results and systematics

These efficiency corrected $\cos \theta^*$ distributions are used to extract the W^\pm helicity fractions. The results of the binned χ^2 fits to these distributions for leptonic and hadronic W decays from the $\sqrt{s}=189$ GeV data are shown in Figure 2. No constraint on the total cross section is applied and one finds that the data are well described only if all three W helicity states are used in the fit. Fits which include only -1 and ± 1 helicities, as also shown in Figure 2, fail to describe the data. For leptonic W decays one finds that the χ^2 increases from 7.1 for seven degrees of freedom if all three W helicity states are included to 17.8 for eight degrees of freedom if only helicity -1 and $+1$ are used to describe the data. For hadronic W decays the χ^2 increases from 9.8 for eight degrees of freedom if all three W helicity states are included to 26.4 for nine degrees of freedom if only helicity ± 1 are used to describe the data.

The fraction of longitudinally polarised W bosons in the $\sqrt{s}=189$ GeV data is measured to be 0.220 ± 0.077 for the leptonic decays and 0.285 ± 0.084 for hadronic decays. The fractions for the different W helicity states, together with the Standard Model Monte Carlo expectations, are given in Table 1 for the $\sqrt{s}=189$ GeV and $\sqrt{s}=183$ GeV data. The observed fractions of longitudinally polarised W bosons measured with leptonic and hadronic W decays agree with each other and with the Standard Model expectation of 0.26 and differ from zero by several standard deviations.

Systematic studies have been performed to verify the stability of the fit results with respect to the fraction of longitudinally polarised W bosons. We have investigated (1) uncertainties due to backgrounds, (2) efficiencies and selection criteria, (3) the hadron energy response functions of the electromagnetic and hadronic calorimeters, (4) the difference between the differential and overall efficiency corrections and (5) a method where the fraction f_0 has been obtained directly from a fit to the measured $\cos \theta^*$ distributions using the Monte Carlo shape from the different W helicity states after the reconstruction.

The analysis has been repeated assuming large relative background uncertainties of $\pm 50\%$ from either the hadronic background or from misidentified $W \rightarrow \tau \nu$ decays. Using these modifications the measured fractions of longitudinally polarised W bosons is found to vary by at most 0.012 for leptonic W decays and by 0.004 for the hadronic W decays. The hadron energy measurement is obtained from a combination of the energy deposited in the electromagnetic and hadron calorimeter multiplied by calibration constants which take the average calorimeter e^\pm /hadron response function into account. These calibration constants have been varied over

a wide range while demanding that the average of the reconstructed masses for leptonic and hadronic W decays agree within better than ± 3 GeV with an average W mass of 80.4 GeV. Since the neutrino momentum vector is reconstructed from the observed missing momentum vector, correlations exist between the reconstructed decay angles in the hadronic W system and the corresponding leptonic W system. For example, a particular choice of the energy calibration constants reduces the fraction of longitudinally polarised W bosons by 0.024 as seen with the leptonic W decays but increases the corresponding fraction for the hadronic decays by 0.015.

Similar variations in the fraction of longitudinally polarised W bosons have been seen with the other systematic studies, as summarised in Table 2. Assuming that the variations given in Table 2 are all due to systematics and adding them in quadrature, a systematic error of ± 0.034 , ± 0.024 and ± 0.016 is assigned to the fraction of longitudinally polarised W bosons measured with leptonic, hadronic decays and for the combined measurement, respectively.

Combining the results from the $\sqrt{s} = 183$ GeV and 189 GeV, ignoring the slight energy dependence of the W helicity fractions expected from the Standard Model, the fraction of longitudinally polarised W bosons is measured to be

$$f_0 = 0.261 \pm 0.051(stat.) \pm 0.016(syst.)$$

and agrees with expectation from the Standard Model of 0.26.

As mentioned in the introduction, it is interesting to measure the W helicity fractions as a function of the W^- scattering angle θ_{W^-} . Thus the fits are repeated for different ranges of $\cos \theta_{W^-}$. The $\cos \theta_{W^-}$ ranges are selected such that the contributions from the transversely polarised W bosons should be either suppressed or enhanced as shown in Figures 3 and 4.

To obtain quantitative numbers for the W helicity fractions as a function of $\cos \theta_{W^-}$ the data from the two different center-of-mass energies are combined and the helicity fractions are measured for three bins of $\cos \theta_{W^-}$. The bins are chosen such that large variations of the different helicity fractions are expected [7] yet keeping a sufficient statistical significance. The results, given in Table 3, agree with the Standard Model expectations and demonstrate that the fraction of W bosons with helicity -1 depends on the W scattering angle as shown in Figure 5.

In summary, all three W boson helicity states, the two transverse as well as the longitudinal ones are observed with fractions in agreement with Standard Model expectations. The production of longitudinally polarised W bosons is thus directly observed with a significance of five standard deviations.

Acknowledgments

We would like to thank F. Jegerlehner, Z. Kunszt, Z. Wąs and D. Zeppenfeld for interesting discussions about the physics of WW production.

We also wish to express our gratitude to the CERN accelerator divisions for the excellent performance of the LEP machine. We acknowledge the contributions of the engineers and technicians who have participated in the construction and maintenance of this experiment.

References

- [1] L3 Collab., M. Acciarri *et al.*, Phys. Lett. **B454** (1999) 386;
L3 Collab., M. Acciarri *et al.*, Phys. Lett. **B436** (1998) 437.
- [2] ALEPH Collab., R. Barate *et al.*, Phys. Lett. **B453** (1999) 121;
ALEPH Collab., R. Barate *et al.*, Phys. Lett. **B453** (1999) 107;
DELPHI Collab., P. Abreu *et al.*, Phys. Lett. **B459** (1999) 382;
DELPHI Collab., P. Abreu *et al.*, Phys. Lett. **B456** (1999) 310;
OPAL Collab., G. Abbiendi *et al.*, Phys. Lett. **B453** (1999) 138;
OPAL Collab., K. Ackerstaff *et al.*, Eur. Phys. J. **C2** (1998) 597.
- [3] OPAL Collab., G. Abbiendi *et al.*, Eur. Phys. J. **C8** (1999) 191.
- [4] S.L. Glashow, Nucl. Phys. **22** (1961) 579;
S. Weinberg, Phys. Rev. Lett. **19** (1967) 1264;
A. Salam, “Elementary Particle Theory”, Ed. N. Svartholm, Stockholm, “Almqvist and Wiksell” (1968), 367.
- [5] M. Veltman, Nucl. Phys. **B7** (1968) 637;
G. ’t Hooft, Nucl. Phys. **B35** (1971) 167;
G. ’t Hooft and M. Veltman, Nucl. Phys. **B44** (1972) 189;
G. ’t Hooft and M. Veltman, Nucl. Phys. **B50** (1972) 318.
- [6] CDF Collab., T. Affolder *et al.*, “Measurement of the Helicity of W Bosons in Top Quark Decays”, Preprint FERMILAB PUB-99/257-E, FERMILAB, 1999, submitted to Phys. Rev. Lett.
- [7] K. Hagiwara, K. Hikasa, R. D. Peccei and D. Zeppenfeld, Nucl. Phys. **B282** (1987) 253.
- [8] L3 Collab., B. Adeva *et al.*, Nucl. Inst. Meth. **A 289** (1990) 35;
L3 Collab., O. Adriani *et al.*, Physics Reports **236** (1993) 1;
I. C. Brock *et al.*, Nucl. Instr. and Meth. **A 381** (1996) 236;
M. Chemarin *et al.*, Nucl. Inst. Meth. **A 349** (1994) 345;
M. Acciarri *et al.*, Nucl. Inst. Meth. **A 351** (1994) 300;
A. Adam *et al.*, Nucl. Inst. Meth. **A 383** (1996) 342;
G. Basti *et al.*, Nucl. Inst. Meth. **A 374** (1996) 293.
- [9] M. Skrzypek, S. Jadach, W. Placzek and Z. Wąs, Comput. Phys. Commun. **94** (1996) 216;
M. Skrzypek, S. Jadach, M. Martinez, W. Placzek and Z. Wąs, Phys. Lett. **B372** (1996) 289.
- [10] J. Fleischer, F. Jegerlehner, K. Kolodziej and G. J. van Oldenborgh, Comput. Phys. Commun. **85** (1995) 29.
- [11] The L3 detector simulation is based on GEANT Version 3.15,
R. Brun *et al.*, *GEANT 3*, CERN-DD/EE/84-1 (Revised), 1987;
and on the GEISHA program to simulate hadronic interactions,
H. Fesefeldt, RWTH Aachen Report PITHA 85/2, 1985.

The L3 Collaboration:

M. Acciarri,²⁶ P. Achard,¹⁹ O. Adriani,¹⁶ M. Aguilar-Benitez,²⁵ J. Alcaraz,²⁵ G. Alemani,²² J. Allaby,¹⁷ A. Aloisio,²⁸ M.G. Alvigi,²⁸ G. Ambrosi,¹⁹ H. Anderhub,⁴⁷ V.P. Andreev,^{6,36} T. Angelescu,¹² F. Anselmo,⁹ A. Arefiev,²⁷ T. Azemoon,³ T. Aziz,¹⁰ P. Bagnaia,³⁵ L. Baksay,⁴² A. Balandras,⁴ R.C. Ball,³ S. Banerjee,¹⁰ Sw. Banerjee,¹⁰ A. Barczyk,^{47,45} R. Barillere,¹⁷ L. Barone,³⁵ P. Bartalini,²² M. Basile,⁹ R. Battiston,³² A. Bay,²² F. Becattini,¹⁶ U. Becker,¹⁴ F. Behner,⁴⁷ L. Bellucci,¹⁶ J. Berdugo,²⁵ P. Berges,¹⁴ B. Bertucci,³² B.L. Betev,⁴⁷ S. Bhattacharya,¹⁰ M. Biasini,³² A. Biland,⁴⁷ J.J. Blaising,⁴ S.C. Blyth,³³ G.J. Bobbink,² A. Böhm,¹ L. Boldizsar,¹³ B. Borgia,³⁵ D. Bourilkov,⁴⁷ M. Bourquin,¹⁹ S. Braccini,¹⁹ J.G. Branson,³⁸ V. Brigljevic,⁴⁷ F. Brochu,⁴ A. Buffini,¹⁶ A. Buijs,⁴³ J.D. Burger,¹⁴ W.J. Burger,³² A. Button,³ X.D. Cai,¹⁴ M. Campanelli,⁴⁷ M. Capell,¹⁴ G. Cara Romeo,⁹ G. Carlino,²⁸ A.M. Cartacci,¹⁶ J. Casaus,²⁵ G. Castellini,¹⁶ F. Cavallari,³⁵ N. Cavallo,²⁸ C. Cecchi,³² M. Cerrada,²⁵ F. Cesaroni,²³ M. Chamizo,¹⁹ Y.H. Chang,⁴⁹ U.K. Chaturvedi,¹⁸ M. Chemarin,²⁴ A. Chen,⁴⁹ G. Chen,⁷ G.M. Chen,⁷ H.F. Chen,²⁰ H.S. Chen,⁷ G. Chiefari,²⁸ L. Cifarelli,³⁷ F. Cindolo,⁹ C. Civinini,¹⁶ I. Clare,¹⁴ R. Clare,¹⁴ G. Coignet,⁴ A.P. Colijn,² N. Colino,²⁵ S. Costantini,⁵ F. Cotorobai,¹² B. Cozzoni,⁹ B. de la Cruz,²⁵ A. Csilling,¹³ S. Cucciarelli,³⁵ T.S. Dai,¹⁴ J.A. van Dalen,³⁰ R.D' Alessandro,¹⁶ R. de Asmundis,¹⁶ P. Déglon,¹⁹ A. Degré,⁴ K. Deiters,⁴⁵ D. della Volpe,²⁸ P. Denes,³⁴ F. DeNotaristefani,³⁵ A. De Salvo,⁴⁷ M. Diemoz,³⁵ D. van Dierendonck,² F. Di Lodovico,⁴⁷ C. Dionisi,³⁵ M. Dittmar,⁴⁷ A. Dominguez,³⁸ A. Doria,²⁸ M.T. Dova,^{18,†} D. Duchesneau,⁴ D. Dufournaud,⁴ P. Duinker,² I. Duran,³⁹ H. El Mamouni,²⁴ A. Engler,³³ F.J. Eppling,¹⁴ F.C. Erné,² P. Extermann,¹⁹ M. Fabre,⁴⁵ R. Faccini,³⁵ M.A. Falagan,²⁵ S. Falciano,^{35,17} A. Favara,¹⁷ J. Fay,²⁴ O. Fedin,³⁶ M. Felcini,⁴⁷ T. Ferguson,³³ F. Ferroni,³⁵ H. Fesefeldt,¹ E. Fiandrini,³² J.H. Field,¹⁹ F. Filthaut,¹⁷ P.H. Fisher,¹⁴ I. Fisk,³⁸ G. Forconi,¹⁴ L. Fredj,¹⁹ K. Freudenreich,⁴⁷ C. Furetta,²⁶ Yu. Galaktionov,^{27,14} S.N. Ganguli,¹⁰ P. Garcia-Abia,⁵ M. Gataullin,³¹ S.S. Gau,¹¹ S. Gentile,^{35,17} N. Gheordanescu,¹² S. Giagu,³⁵ Z.F. Gong,²⁰ G. Grenier,²⁴ O. Grimm,⁴⁷ M.W. Gruenewald,⁸ M. Guida,³⁷ R. van Gulik,² V.K. Gupta,³⁴ A. Gurtu,¹⁰ L.J. Gutay,⁴⁴ D. Haas,⁵ A. Hasan,²⁹ D. Hatzifotiadou,⁹ T. Hebbeker,⁸ A. Hervé,¹⁷ P. Hidas,¹³ J. Hirschfelder,³³ H. Hofer,⁴⁷ G. Holzner,⁴⁷ H. Hoorani,³³ S.R. Hou,⁴⁹ I. Iashvili,⁴⁶ B.N. Jin,⁷ L.W. Jones,³ P. de Jong,² I. Josa-Mutuberría,²⁵ R.A. Khan,¹⁸ M. Kaur,^{18,◇} M.N. Kienzle-Focacci,¹⁹ D. Kim,³⁵ D.H. Kim,⁴¹ J.K. Kim,⁴¹ S.C. Kim,⁴¹ J. Kirkby,¹⁷ D. Kiss,¹³ W. Kittel,³⁰ A. Klimentov,^{14,27} A.C. König,³⁰ A. Kopp,⁴⁶ V. Koutsenko,^{14,27} M. Kräber,⁴⁷ R.W. Kraemer,³³ W. Krenz,¹ A. Krüger,⁴⁶ A. Kunin,^{14,27} P. Ladrón de Guevara,²⁵ I. Laktineh,²⁴ G. Landi,¹⁶ K. Lassila-Perini,⁴⁷ M. Lebeau,¹⁷ A. Lebedev,¹⁴ P. Lebrun,²⁴ P. Lecomte,⁴⁷ P. Lecoq,¹⁷ P. Le Coultre,⁴⁷ H.J. Lee,⁸ J.M. Le Goff,¹⁷ R. Leiste,⁴⁶ E. Leonardi,³⁵ P. Levchenko,³⁶ C. Li,²⁰ S. Likhoded,⁴⁶ C.H. Lin,⁴⁹ W.T. Lin,⁴⁹ F.L. Linde,² L. Lista,²⁸ Z.A. Liu,⁷ W. Lohmann,⁴⁶ E. Longo,³⁵ Y.S. Lu,⁷ K. Lübelmeyer,¹ C. Luci,^{17,35} D. Luckey,¹⁴ L. Lugnier,²⁴ L. Luminari,³⁵ W. Lustermaier,⁴⁷ W.G. Ma,²⁰ M. Maity,¹⁰ L. Malgeri,¹⁷ A. Malinin,¹⁷ C. Mañá,²⁵ D. Mangeol,³⁰ P. Marchesini,⁴⁷ G. Marian,¹⁵ J.P. Martin,²⁴ F. Marzano,³⁵ G.G.G. Massaro,² K. Mazumdar,¹⁰ R.R. McNeil,⁶ S. Mele,¹⁷ L. Merola,²⁸ M. Meschini,¹⁶ W.J. Metzger,³⁰ M. von der Mey,¹ A. Mihul,¹² H. Milcent,¹⁷ G. Mirabelli,³⁵ J. Mnich,¹⁷ G.B. Mohanty,¹⁰ P. Molnar,⁸ B. Monteleoni,^{16,†} T. Moulik,¹⁰ G.S. Muanza,²⁴ F. Muheim,¹⁹ A.J.M. Muijs,² M. Musy,³⁵ M. Napolitano,²⁸ F. Nessi-Tedaldi,⁴⁷ H. Newman,³¹ T. Niessen,¹ A. Nisati,³⁵ H. Nowak,⁴⁶ Y.D. Oh,⁴¹ G. Organtini,³⁵ A. Oulianov,²⁷ C. Palomares,²⁵ D. Pandoulas,¹ S. Paoletti,^{35,17} P. Paolucci,²⁸ R. Paramatti,³⁵ H.K. Park,³³ I.H. Park,⁴¹ G. Pascale,³⁵ G. Passaleva,¹⁷ S. Patricelli,²⁸ T. Paul,¹¹ M. Pauluzzi,³² C. Paus,¹⁷ F. Pauss,⁴⁷ M. Pedace,³⁵ S. Pensotti,²⁶ D. Perret-Gallix,⁴ B. Petersen,³⁰ D. Piccolo,²⁸ F. Pierella,⁹ M. Pieri,¹⁶ P.A. Piroué,³⁴ E. Pistolesi,²⁶ V. Plyaskin,²⁷ M. Pohl,¹⁹ V. Pojidaev,^{27,16} H. Postema,¹⁴ J. Pothier,¹⁷ N. Produit,¹⁹ D.O. Prokofiev,⁴⁴ D. Prokofiev,³⁶ J. Quartieri,³⁷ G. Rahal-Callot,^{47,17} M.A. Rahaman,¹⁰ P. Raics,¹⁵ N. Raja,¹⁰ R. Ramelli,⁴⁷ P.G. Rancoita,²⁶ A. Raspereza,⁴⁶ G. Raven,³⁸ P. Razis,²⁹ D. Ren,⁴⁷ M. Rescigno,³⁵ S. Reucroft,¹¹ T. van Rhee,⁴³ S. Riemann,⁴⁶ K. Riles,³ A. Robohm,⁴⁷ J. Rodin,⁴² B.P. Roe,³ L. Romero,²⁵ A. Rosca,⁸ S. Rosier-Lees,⁴ J.A. Rubio,¹⁷ D. Ruschmeier,⁸ H. Rykaczewski,⁴⁷ S. Saremi,⁶ S. Sarkar,³⁵ J. Salicio,¹⁷ E. Sanchez,¹⁷ M.P. Sanders,³⁰ M.E. Sarakinos,²¹ C. Schäfer,¹⁷ V. Schegelsky,³⁶ S. Schmidt-Kaerst,¹ D. Schmitz,¹ H. Schopper,⁴⁸ D.J. Schotanus,³⁰ G. Schwering,¹ C. Sciacca,²⁸ D. Sciarrino,¹⁹ A. Seganti,⁹ L. Servoli,³² S. Shevchenko,³¹ N. Shivarov,⁴⁰ V. Shoutko,²⁷ E. Shumilov,²⁷ A. Shvorob,³¹ T. Siedenburger,¹ D. Son,⁴¹ B. Smith,³³ P. Spillantini,¹⁶ M. Steuer,¹⁴ D.P. Stickland,³⁴ A. Stone,⁶ H. Stone,^{34,†} B. Stoyanov,⁴⁰ A. Straessner,¹ K. Sudhakar,¹⁰ G. Sultanov,¹⁸ L.Z. Sun,²⁰ H. Suter,⁴⁷ J.D. Swain,¹⁸ Z. Szillasi,^{42,¶} T. Sztaricskai,^{42,¶} X.W. Tang,⁷ L. Tauscher,⁵ L. Taylor,¹¹ C. Timmermans,³⁰ Samuel C.C. Ting,¹⁴ S.M. Ting,¹⁴ S.C. Tonwar,¹⁰ J. Tóth,¹³ C. Tully,¹⁷ K.L. Tung,⁷ Y. Uchida,¹⁴ J. Ulbricht,⁴⁷ E. Valente,³⁵ G. Vesztegombi,¹³ I. Vetlitsky,²⁷ D. Vicinanza,³⁷ G. Viertel,⁴⁷ S. Villa,¹¹ M. Vivargent,⁴ S. Vlachos,⁵ I. Vodopianov,³⁶ H. Vogel,³³ H. Vogt,⁴⁶ I. Vorobiev,²⁷ A.A. Vorobyov,³⁶ A. Vorvolakos,²⁹ M. Wadhwa,⁵ W. Wallraff,¹ M. Wang,¹⁴ X.L. Wang,²⁰ Z.M. Wang,²⁰ A. Weber,¹ M. Weber,¹ P. Wienemann,¹ H. Wilkens,³⁰ S.X. Wu,¹⁴ S. Wynhoff,¹⁷ L. Xia,³¹ Z.Z. Xu,²⁰ B.Z. Yang,²⁰ C.G. Yang,⁷ H.J. Yang,⁷ M. Yang,⁷ J.B. Ye,²⁰ S.C. Yeh,⁵⁰ An. Zalite,³⁶ Yu. Zalite,³⁶ Z.P. Zhang,²⁰ G.Y. Zhu,⁷ R.Y. Zhu,³¹ A. Zichichi,^{9,17,18} G. Zilizi,^{42,¶} M. Zöller,¹

- 1 I. Physikalisches Institut, RWTH, D-52056 Aachen, FRG[§]
III. Physikalisches Institut, RWTH, D-52056 Aachen, FRG[§]
 - 2 National Institute for High Energy Physics, NIKHEF, and University of Amsterdam, NL-1009 DB Amsterdam, The Netherlands
 - 3 University of Michigan, Ann Arbor, MI 48109, USA
 - 4 Laboratoire d'Annecy-le-Vieux de Physique des Particules, LAPP, IN2P3-CNRS, BP 110, F-74941 Annecy-le-Vieux CEDEX, France
 - 5 Institute of Physics, University of Basel, CH-4056 Basel, Switzerland
 - 6 Louisiana State University, Baton Rouge, LA 70803, USA
 - 7 Institute of High Energy Physics, IHEP, 100039 Beijing, China[△]
 - 8 Humboldt University, D-10099 Berlin, FRG[§]
 - 9 University of Bologna and INFN-Sezione di Bologna, I-40126 Bologna, Italy
 - 10 Tata Institute of Fundamental Research, Bombay 400 005, India
 - 11 Northeastern University, Boston, MA 02115, USA
 - 12 Institute of Atomic Physics and University of Bucharest, R-76900 Bucharest, Romania
 - 13 Central Research Institute for Physics of the Hungarian Academy of Sciences, H-1525 Budapest 114, Hungary[‡]
 - 14 Massachusetts Institute of Technology, Cambridge, MA 02139, USA
 - 15 KLTE-ATOMKI, H-4010 Debrecen, Hungary[¶]
 - 16 INFN Sezione di Firenze and University of Florence, I-50125 Florence, Italy
 - 17 European Laboratory for Particle Physics, CERN, CH-1211 Geneva 23, Switzerland
 - 18 World Laboratory, FBLJA Project, CH-1211 Geneva 23, Switzerland
 - 19 University of Geneva, CH-1211 Geneva 4, Switzerland
 - 20 Chinese University of Science and Technology, USTC, Hefei, Anhui 230 029, China[△]
 - 21 SEFT, Research Institute for High Energy Physics, P.O. Box 9, SF-00014 Helsinki, Finland
 - 22 University of Lausanne, CH-1015 Lausanne, Switzerland
 - 23 INFN-Sezione di Lecce and Università Degli Studi di Lecce, I-73100 Lecce, Italy
 - 24 Institut de Physique Nucléaire de Lyon, IN2P3-CNRS, Université Claude Bernard, F-69622 Villeurbanne, France
 - 25 Centro de Investigaciones Energéticas, Medioambientales y Tecnológicas, CIEMAT, E-28040 Madrid, Spain^b
 - 26 INFN-Sezione di Milano, I-20133 Milan, Italy
 - 27 Institute of Theoretical and Experimental Physics, ITEP, Moscow, Russia
 - 28 INFN-Sezione di Napoli and University of Naples, I-80125 Naples, Italy
 - 29 Department of Natural Sciences, University of Cyprus, Nicosia, Cyprus
 - 30 University of Nijmegen and NIKHEF, NL-6525 ED Nijmegen, The Netherlands
 - 31 California Institute of Technology, Pasadena, CA 91125, USA
 - 32 INFN-Sezione di Perugia and Università Degli Studi di Perugia, I-06100 Perugia, Italy
 - 33 Carnegie Mellon University, Pittsburgh, PA 15213, USA
 - 34 Princeton University, Princeton, NJ 08544, USA
 - 35 INFN-Sezione di Roma and University of Rome, "La Sapienza", I-00185 Rome, Italy
 - 36 Nuclear Physics Institute, St. Petersburg, Russia
 - 37 University and INFN, Salerno, I-84100 Salerno, Italy
 - 38 University of California, San Diego, CA 92093, USA
 - 39 Dept. de Física de Partículas Elementales, Univ. de Santiago, E-15706 Santiago de Compostela, Spain
 - 40 Bulgarian Academy of Sciences, Central Lab. of Mechatronics and Instrumentation, BU-1113 Sofia, Bulgaria
 - 41 Center for High Energy Physics, Adv. Inst. of Sciences and Technology, 305-701 Taejeon, Republic of Korea
 - 42 University of Alabama, Tuscaloosa, AL 35486, USA
 - 43 Utrecht University and NIKHEF, NL-3584 CB Utrecht, The Netherlands
 - 44 Purdue University, West Lafayette, IN 47907, USA
 - 45 Paul Scherrer Institut, PSI, CH-5232 Villigen, Switzerland
 - 46 DESY, D-15738 Zeuthen, FRG
 - 47 Eidgenössische Technische Hochschule, ETH Zürich, CH-8093 Zürich, Switzerland
 - 48 University of Hamburg, D-22761 Hamburg, FRG
 - 49 National Central University, Chung-Li, Taiwan, China
 - 50 Department of Physics, National Tsing Hua University, Taiwan, China
- [§] Supported by the German Bundesministerium für Bildung, Wissenschaft, Forschung und Technologie
[‡] Supported by the Hungarian OTKA fund under contract numbers T019181, F023259 and T024011.
[¶] Also supported by the Hungarian OTKA fund under contract numbers T22238 and T026178.
^b Supported also by the Comisión Interministerial de Ciencia y Tecnología.
[‡] Also supported by CONICET and Universidad Nacional de La Plata, CC 67, 1900 La Plata, Argentina.
[◇] Also supported by Panjab University, Chandigarh-160014, India.
[△] Supported by the National Natural Science Foundation of China.
[†] Deceased.

| $\sqrt{s} = 189 \text{ GeV}$ | | | | | |
|------------------------------|----------------------------------|-------------------|-------------------|---|-------------------|
| | Helicity $W \rightarrow \ell\nu$ | | | Helicity $W \rightarrow \text{hadrons}$ | |
| | -1 | +1 | 0 | ± 1 | 0 |
| Data | 0.568 ± 0.071 | 0.212 ± 0.046 | 0.220 ± 0.077 | 0.716 ± 0.086 | 0.285 ± 0.084 |
| MC | 0.56 | 0.18 | 0.26 | 0.74 | 0.26 |
| $\sqrt{s} = 183 \text{ GeV}$ | | | | | |
| Data | 0.56 ± 0.14 | 0.10 ± 0.08 | 0.34 ± 0.15 | 0.75 ± 0.17 | 0.25 ± 0.17 |
| MC | 0.53 | 0.20 | 0.27 | 0.73 | 0.27 |

Table 1: Measured W helicity fractions for the leptonic and hadronic W decays for the $\sqrt{s} = 189 \text{ GeV}$ and $\sqrt{s} = 183 \text{ GeV}$ data samples. The corresponding helicity fractions in the Standard Model as implemented in the KORALW Monte Carlo program where the statistical errors are negligible in comparison with the data are also given.

| Fraction of longitudinally polarised W bosons | | | |
|---|-------------------------|--------------------------------|-------------------|
| | $W \rightarrow \ell\nu$ | $W \rightarrow \text{hadrons}$ | average |
| standard method | 0.220 ± 0.077 | 0.285 ± 0.084 | 0.252 ± 0.057 |
| background corrections | 0.209–0.232 | 0.282–0.286 | 0.241–0.258 |
| efficiency uncertainty | 0.214 | 0.279 | 0.247 |
| calorimeter calibration (hadrons) | 0.197–0.215 | 0.282–0.300 | 0.244–0.254 |
| integrated efficiency correction | 0.233 | 0.268 | 0.250 |
| analysis method | 0.237 | 0.279 | 0.258 |

Table 2: Measurements of the fraction of longitudinally polarised W bosons for leptonic and hadronic W decays from the $\sqrt{s} = 189$ GeV data sample investigating various sources of systematics.

| $\sqrt{s} = 183 + 189 \text{ GeV data}$ | | | | | |
|--|----------------------------------|-----------------|-----------------|---|-----------------|
| | Helicity $W \rightarrow \ell\nu$ | | | Helicity $W \rightarrow \text{hadrons}$ | |
| $\cos \theta_{W^-}$ | -1 | +1 | 0 | ± 1 | 0 |
| -1.0 - -0.4 | 0.27 ± 0.12 | 0.45 ± 0.22 | 0.28 ± 0.23 | 0.87 ± 0.28 | 0.13 ± 0.28 |
| -0.4 - 0.3 | 0.40 ± 0.09 | 0.23 ± 0.08 | 0.37 ± 0.12 | 0.94 ± 0.16 | 0.06 ± 0.15 |
| 0.3 - 1.0 | 0.66 ± 0.08 | 0.08 ± 0.04 | 0.26 ± 0.08 | 0.75 ± 0.11 | 0.23 ± 0.10 |
| $\sqrt{s} = 183 + 189 \text{ GeV KORALW MC}$ | | | | | |
| | Helicity $W \rightarrow \ell\nu$ | | | Helicity $W \rightarrow \text{hadrons}$ | |
| $\cos \theta_{W^-}$ | -1 | +1 | 0 | ± 1 | 0 |
| -1.0 - -0.4 | 0.13 | 0.45 | 0.42 | 0.58 | 0.42 |
| -0.4 - 0.3 | 0.42 | 0.29 | 0.29 | 0.71 | 0.29 |
| 0.3 - 1.0 | 0.67 | 0.10 | 0.23 | 0.77 | 0.23 |

Table 3: Same as Table 1, except in this case the helicity fractions are given as a function of $\cos \theta_{W^-}$ and combining the $\sqrt{s} = 183 \text{ GeV}$ and $\sqrt{s} = 189 \text{ GeV}$ data and Monte Carlo.

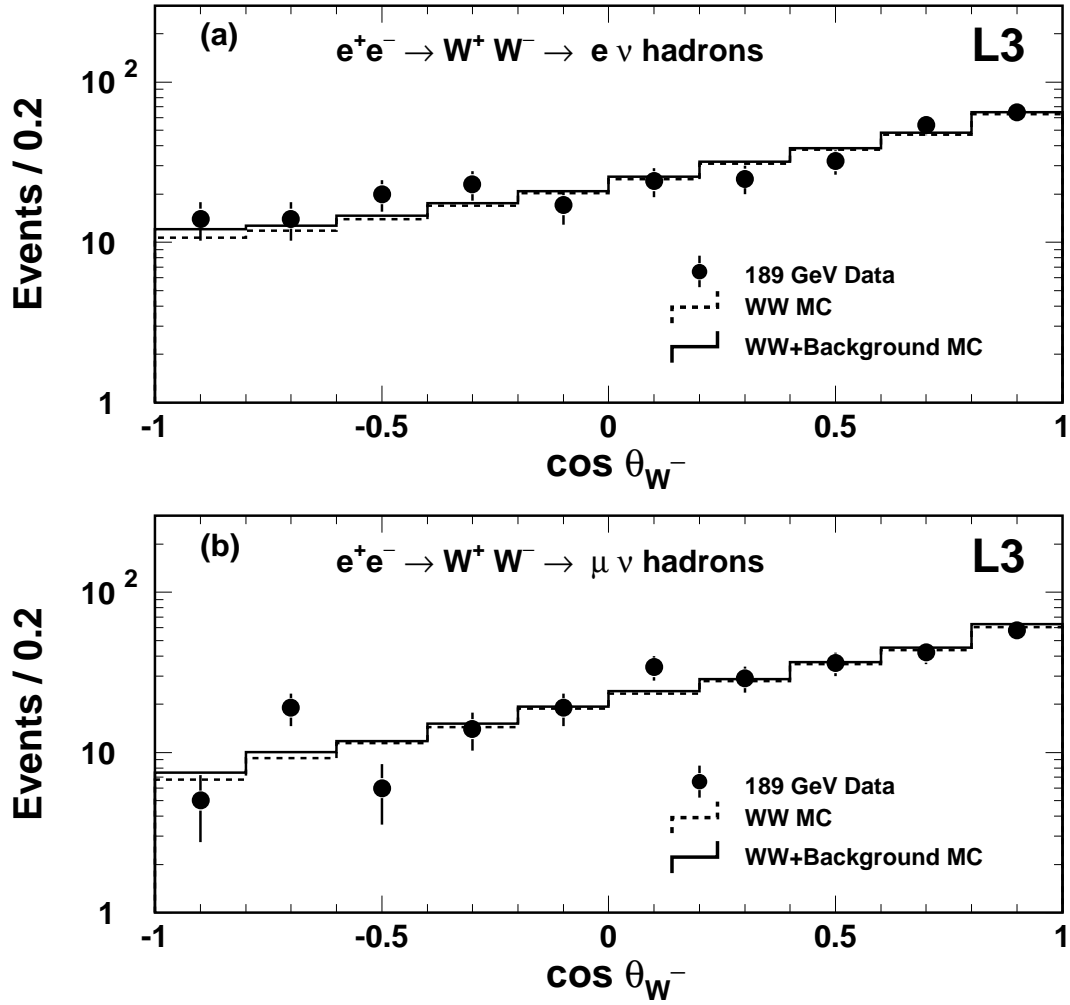


Figure 1: The $\cos \theta_{W^-}$ distribution for (a) $W^+W^- \rightarrow e\nu q\bar{q}$ and (b) $W^+W^- \rightarrow \mu\nu q\bar{q}$ events from the $\sqrt{s} = 189$ GeV data (points) and the KORALW Monte Carlo prediction (histogram).

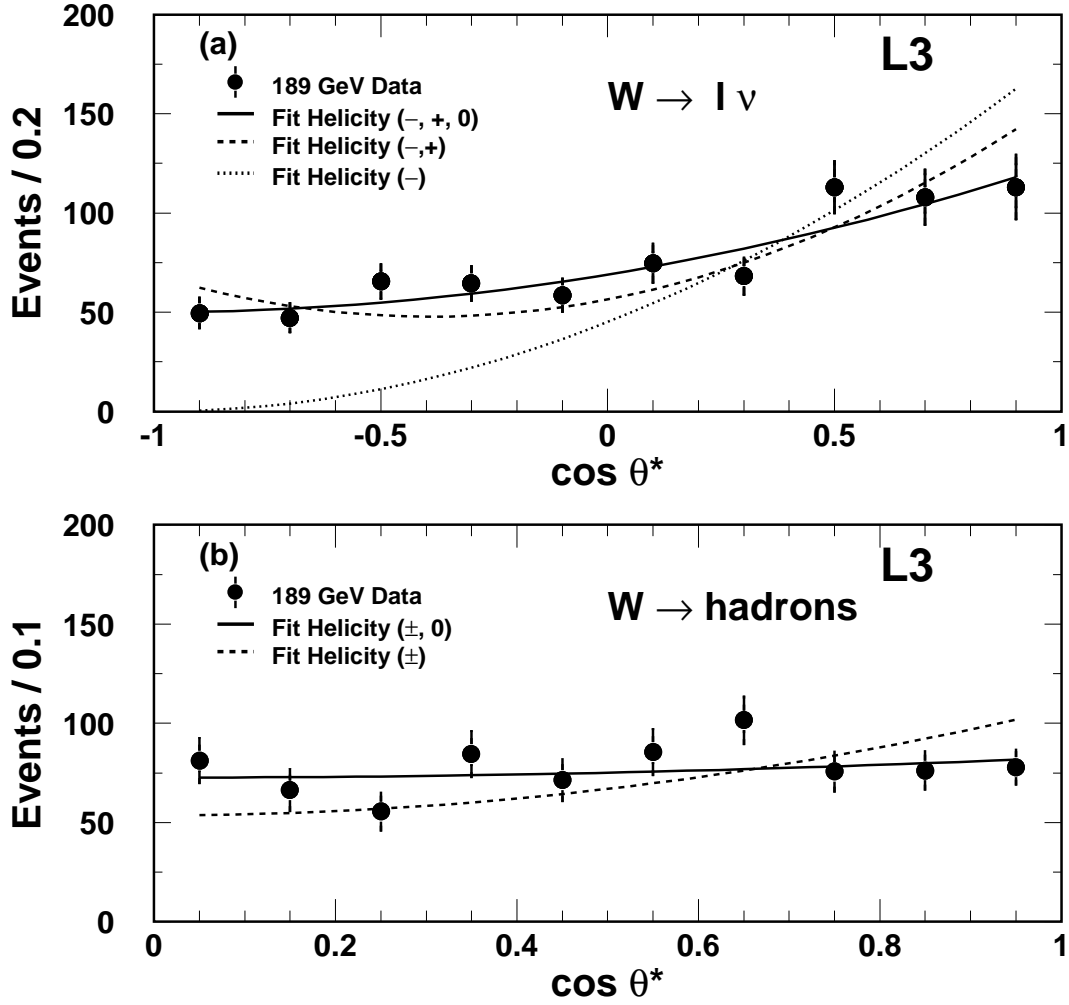


Figure 2: Efficiency- and background-corrected $\cos \theta^*$ distributions for (a) leptonic W decays and (b) for hadronic W decays at $\sqrt{s} = 189$ GeV. The fit results for the different W helicity hypotheses are also shown.

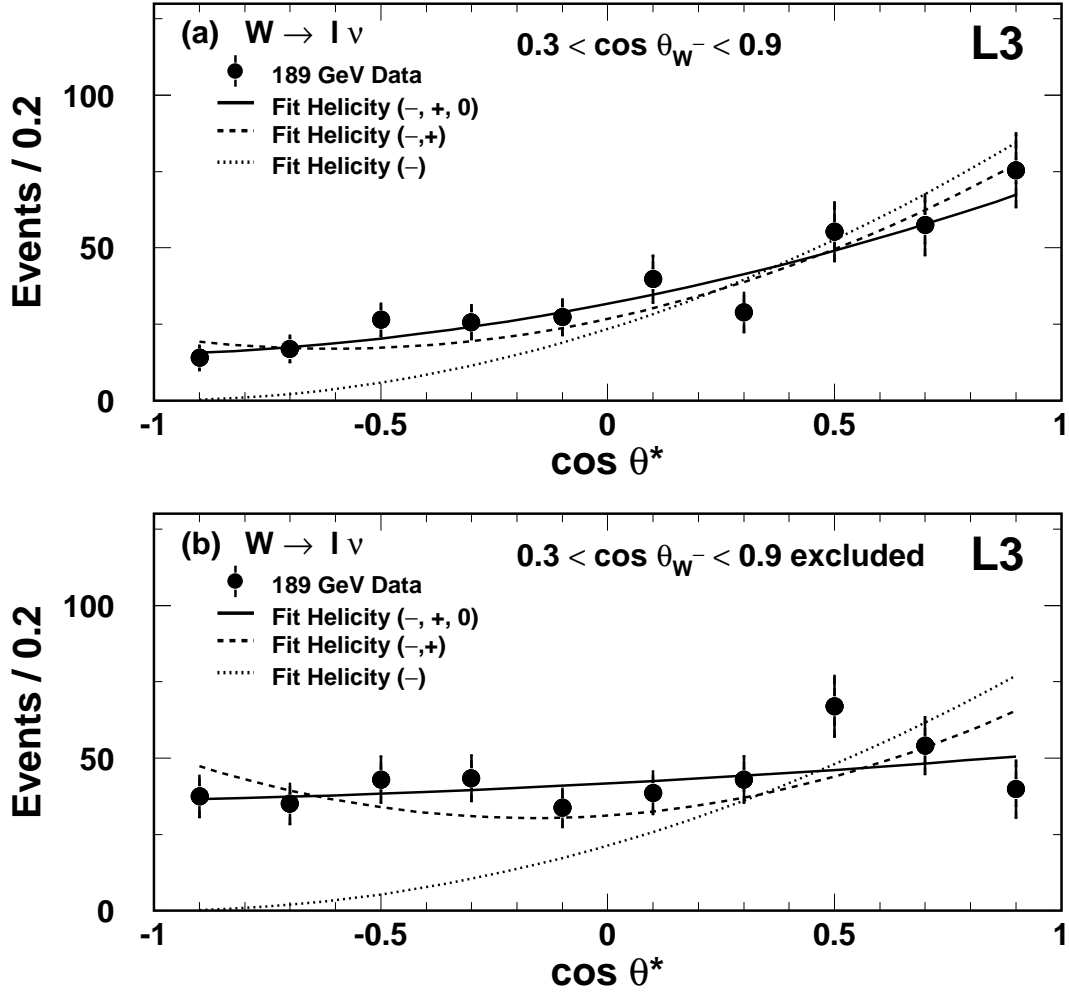


Figure 3: Corrected $\cos \theta^*$ distribution from leptonic W decays for (a) enriched and (b) depleted transverse W polarisation regions together with the fit results. For (a) the required θ_{W^-} must satisfy $0.3 < \cos \theta_{W^-} < 0.9$, while for (b) it has to be $\cos \theta_{W^-} < 0.3$ or $0.9 < \cos \theta_{W^-}$.

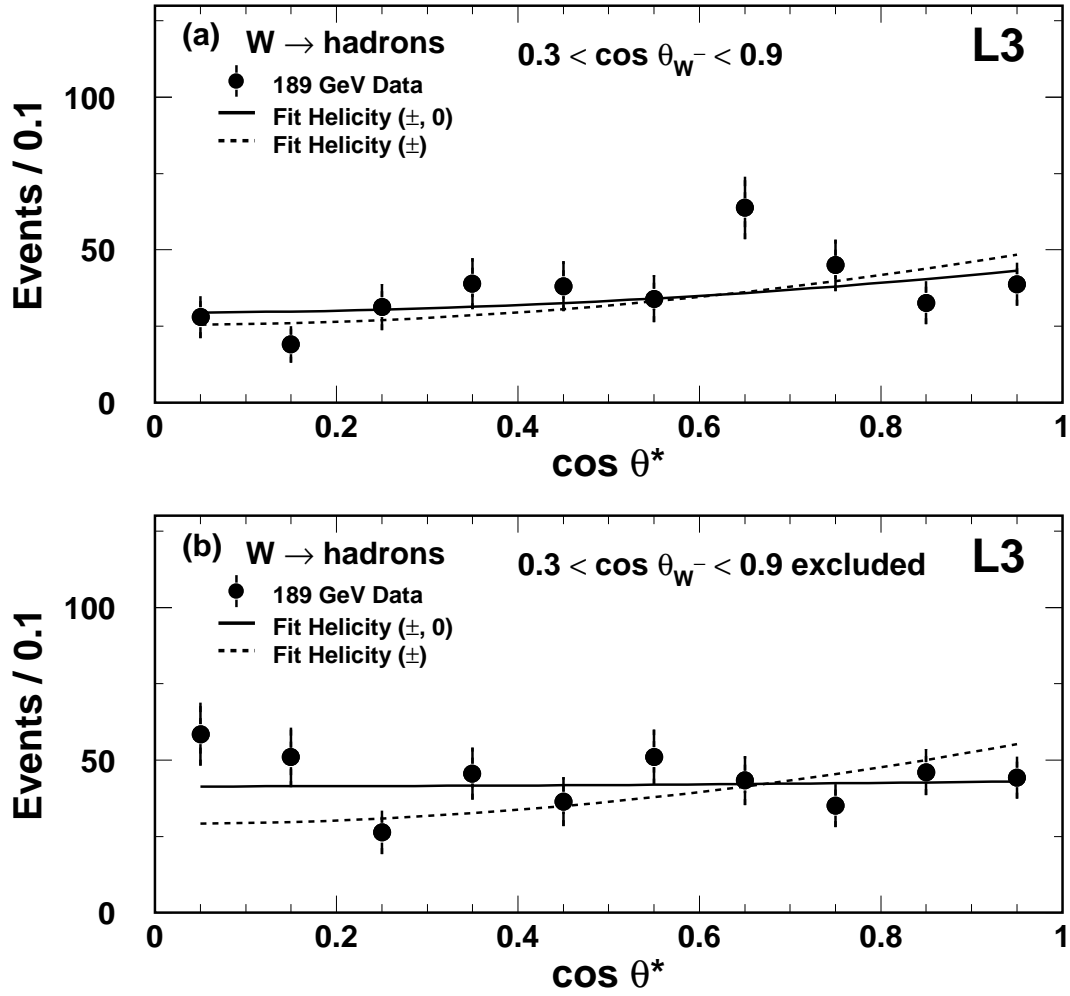


Figure 4: Same as Figure 3 except that in this case $|\cos \theta^*|$ is shown for hadronic W decays.

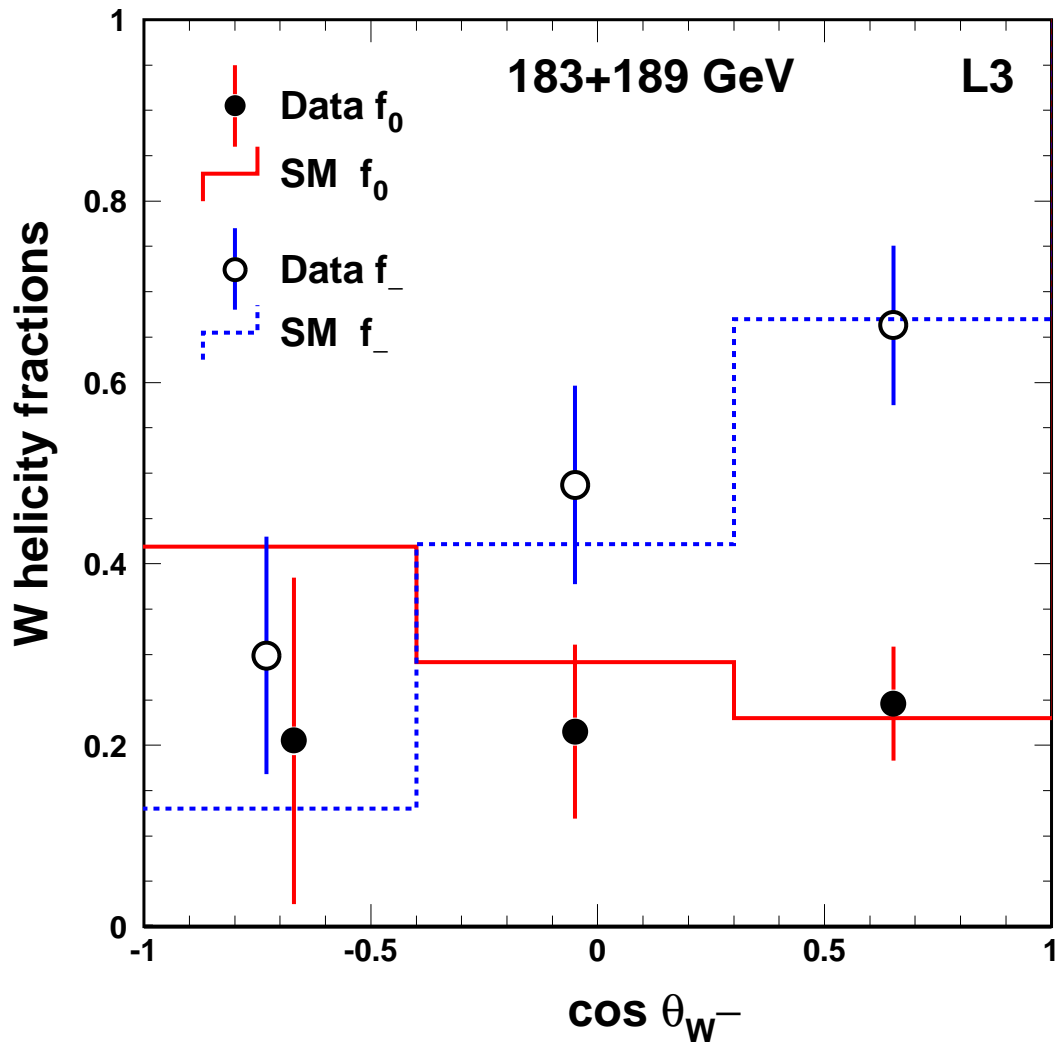


Figure 5: W helicity fractions f_0 and f_- for three different bins of $\cos \theta_{W^-}$ in the combined data sample and in the KORALW Monte Carlo.